Applied Mathematics Letters 146 (2023) 108821

Contents lists available at ScienceDirect

Applied Mathematics Letters

www.elsevier.com/locate/aml

Exotic dynamics of bimolecular reaction–diffusion fronts in immiscible systems

S.C. Generalis [a], A. De Wit [b], P.M.J. Trevelyan [a,*]

[a] *Department of Applied Mathematics and Data Science, Aston University, B4 7ET Birmingham, UK*
[b] *Nonlinear Physical Chemistry Unit, Université Libre de Bruxelles (ULB), CP 231 1050 Brussels, Belgium*

ARTICLE INFO

Article history:
Received 7 June 2023
Received in revised form 4 August 2023
Accepted 4 August 2023
Available online 9 August 2023

Keywords:
Chemical front
Reaction-diffusion
Interface
Small time asymptotics
Mass transfer

ABSTRACT

Dynamics of bimolecular A+B→C reaction-diffusion (RD) fronts have been well characterized in miscible systems. We study here their properties when reactants A and B are initially dissolved in two immiscible solvents put in contact. Neglecting any convective effects, we show that bimolecular RD fronts developing in such immiscible systems upon transfer from the reactants from one phase to the other can change directions up to four times, contrary to miscible systems where only two changes of direction are possible. Further, the conditions for which two local maxima in the reaction rate can exist are identified.

1. Introduction

Bimolecular A+B→C reaction-diffusion fronts are commonly observed in a wealth of different dynamic systems ranging from geology [1], biology [2] to economy [3], to name a few. Numerous theoretical studies have characterized the properties of such fronts including that, for large times, the reaction front moves like the square root of time and has a width of the order of time to the power of one sixth [4–12]. To validate these theoretical studies, experiments have been typically carried out in gels or very thin capillaries by putting in contact two miscible solutions of reactants A and B and following the dynamics of the product formed in the contact zone [13–16]. These experiments have validated the theoretical scalings and have also evidenced that the position of the bimolecular chemical reaction front can change directions once [14]. This position is often defined as the position X_f where the reaction rate $R = kAB$, with A and B the concentrations of the respective reactant, reaches its maximum or, as in this work, the position of the first moment of the

* Corresponding author.
E-mail address: p.trevelyan@aston.ac.uk (P.M.J. Trevelyan).

https://doi.org/10.1016/j.aml.2023.108821

production rate [17], namely

$$X_f = \frac{\int_{-\infty}^{\infty} RX dX}{\int_{-\infty}^{\infty} R dX}, \tag{1}$$

where X is the Cartesian one dimensional distance from the gel interface.

For finite systems, complex dynamics can emerge [18] and, in particular, the position of the reaction front can change directions twice in the miscible case when the diffusion coefficients of species A and B are unequal [19–21]. For this miscible case, a bifurcation diagram in the parameter space has identified the number of times the reaction front changes direction [22].

The case of immiscible systems has, however, been less studied. In such systems, two different immiscible solvents, each containing one of the A or B reactants are put in contact and A+B→C reaction-diffusion fronts can then develop only after transfer of the reactants from one phase to the other. The problem is more complex as a partition coefficient controlling the jump in concentrations at the interface due to variable solubility in each solvent has to be introduced. Moreover, the A and B species may have different diffusion coefficients in each solvent which enlarges the parameter space. Experiments show that complex convective dynamics can be observed in solutions [23–27]. There is thus a need to analyse the properties of the underlying RD A+B→C fronts to understand the specific new properties that the immiscible character of the problem brings before studying the effect of convection.

In this context, we analyse here theoretically the properties of A+B→C reaction-diffusion fronts in immiscible systems. In particular, using small and large time asymptotic results along with numerical solutions, we examine the number of times a reaction front can change directions. We find that, in immiscible systems, the front can change directions up to four times, which shows the rich new possible dynamics introduced by transfer properties between two different phases. We characterize the RD concentration profiles as a function of the parameters and delineate in the parameter space the possible number of direction changes that such fronts can feature.

2. Physical model

Consider the case of two immiscible solutions placed next to each other at a planar interface located at $X = 0$ for time $T \geq 0$. Each solvent contains a different reactant, either A or B. These reactants A and B meet by transfer between the immiscible solvents at the contact line followed by diffusion and reaction according to a bimolecular $A + B \to C$ reaction. The product C will be ignored in the model as it does not affect the position of the reaction front. We shall use superscript notation $A^{(i)}$ and $B^{(i)}$ to distinguish between the two solutions with $i = 1$ denoting the left solution initially containing A ($X < 0$) and $i = 2$ denoting the right solution where B is initially dissolved ($X > 0$). Hence we have the separated homogeneous initial conditions

$$A^{(1)} = A_0, \quad B^{(1)} = 0 \quad \text{for} \quad X < 0 \tag{2a}$$

$$A^{(2)} = 0, \quad B^{(2)} = B_0 \quad \text{for} \quad X > 0 \tag{2b}$$

where A_0 and B_0 are the initial concentrations of reactants A and B, respectively. The mean field approximation is assumed and the rate of reaction is thus given by $R = k^{(i)} A^{(i)} B^{(i)}$. The kinetic constants $k^{(1)}$ and $k^{(2)}$ are constants that depend on the gel. Neglecting any convection, this model can be expressed as the following system of one-dimensional reaction-diffusion equations:

$$A_T^{(i)} = D_a^{(i)} A_{XX}^{(i)} - k^{(i)} A^{(i)} B^{(i)}, \tag{2c}$$

$$B_T^{(i)} = D_b^{(i)} B_{XX}^{(i)} - k^{(i)} A^{(i)} B^{(i)}. \tag{2d}$$

The reactant concentrations in the immiscible solutions are considered to be sufficiently dilute that the molecular diffusion coefficients $D_a^{(i)}$ and $D_b^{(i)}$ can be assumed constant but different in each solution. The subscripts X and T denote partial derivatives with respect to space and time.

The difference between the solubility of A and B in each solvent can be characterized by partition coefficients p_a and p_b which are constant at equilibrium. We assume that the transition of chemical species between the two phases is fast enough such that adsorption and desorption kinetics can be neglected and the partition coefficient can be taken as a constant at the interface, hence at $X = 0$ we have

$$p_a = \frac{A^{(1)}}{A^{(2)}}, \quad p_b = \frac{B^{(1)}}{B^{(2)}}. \tag{2e}$$

The interfacial flux balances are given by

$$D_a^{(1)} A_X^{(1)} = D_a^{(2)} A_X^{(2)}, \quad D_b^{(1)} B_X^{(1)} = D_b^{(2)} B_X^{(2)}. \tag{2f}$$

The domain is considered sufficiently large that it can be treated as infinite, so we apply no flux far field conditions:

$$A_X^{(1)}, B_X^{(1)} \to 0 \quad \text{as} \quad X \to -\infty, \tag{2g}$$
$$A_X^{(2)}, B_X^{(2)} \to 0 \quad \text{as} \quad X \to \infty\,. \tag{2h}$$

We non-dimensionalize this problem with the characteristic time and length scales using the kinetic constant and diffusion coefficient of reactant A in solution 2, i.e.

$$t_0 = \frac{1}{k^{(2)} A_0} \quad \text{and} \quad l_0 = \sqrt{D_a^{(2)} t_0}. \tag{3}$$

We introduce the dimensionless variables $x = X/l_0$, $t = T/t_0$, $a = A/A_0$ and $b = B/A_0$ and dimensionless parameters

$$\phi = \frac{B_0}{A_0}, \ \kappa = \frac{k^{(1)}}{k^{(2)}}, \ q = \sqrt{\frac{D_a^{(2)}}{D_a^{(1)}}}, \ r = \sqrt{\frac{D_a^{(2)}}{D_b^{(2)}}}, \ \hat{r} = \sqrt{\frac{D_a^{(2)}}{D_b^{(1)}}},$$

where ϕ represents the initial reactant concentration ratio, κ is the ratio of the kinetic constants and q, r and $\hat{r}$ are the square root of the diffusion coefficient ratios. It is then useful to transform the problem from (x, t) to (η, t) using the similarity variable

$$\eta = \frac{x}{\sqrt{4t}}.$$

3. Asymptotic limits

3.1. Small time asymptotic limit

In the small time asymptotic limit we obtain

$$\Gamma^{(i)} = \Gamma_0^{(i)}(\eta) + \mathcal{O}(t) \tag{4}$$

where i equals 1 or 2 and Γ represents a or b. The zeroth order solutions are given by [28]:

$$a_0^{(1)} = 1 - \frac{\operatorname{erfc}(-q\eta)}{1 + p_a q^{-1}}, \quad a_0^{(2)} = \frac{\operatorname{erfc}(\eta)}{p_a + q}, \quad b_0^{(1)} = \frac{\phi \operatorname{erfc}(-\hat{r}\eta)}{p_b^{-1} + r\hat{r}^{-1}}, \quad b_0^{(2)} = \phi - \frac{\phi \operatorname{erfc}(r\eta)}{1 + p_b^{-1}\hat{r}r^{-1}}. \tag{5}$$

Note that these zeroth order concentration profiles for immiscible solutions depend on the six variables p_a, p_b, q, r, $\hat{r}$ and ϕ.

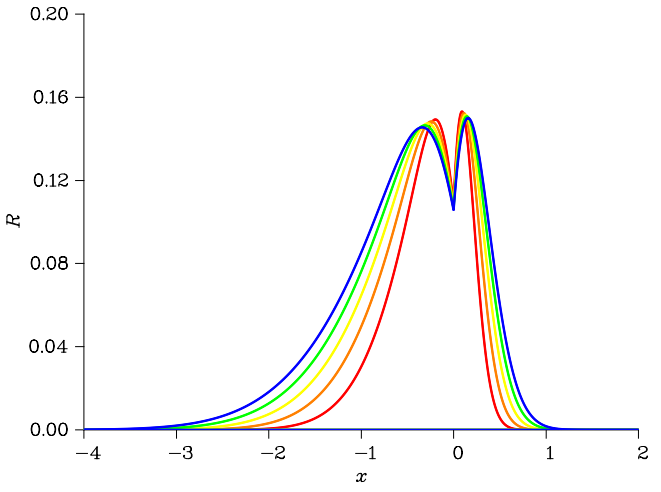

Fig. 1. Profiles of the reaction rate R against x illustrating two local maxima when $\kappa = \phi = p_a = p_b = r = 1$, $q = 1.1$ and $\hat{r} = 0.3$, at times $t = 0.02$ (red), 0.04 (orange), 0.06 (yellow), 0.08 (green) and 0.1 (blue).

3.2. Small time maximum reaction rate

The position where the reaction rate R is maximum was referred to as x_m by [22] in miscible systems. However, in immiscible systems, using the small time asymptotic solutions in Eqs. (5), it is found that there can be up to two local maxima in the reaction rate. Therefore for clarity we use $x_m^{(i)}$ to denote the position of the maximum local reaction rate in each solution. In solution 1, if $\hat{r}^{-1} \geq p_a q^{-2}$, then the position of the reaction front is $x_m^{(1)} = 2\alpha_1\sqrt{t}$ where α_1 satisfies

$$q e^{\hat{r}^2\alpha_1^2}\mathrm{erfc}(-\hat{r}\alpha_1) = \hat{r} e^{q^2\alpha_1^2}\left[p_a q^{-1} + \mathrm{erf}(-q\alpha_1)\right], \tag{6}$$

otherwise no local maximum in the reaction rate occurs in zone 1. In solution 2, if $p_b \geq \hat{r} r^{-2}$, then the position of the reaction front is $x_m^{(2)} = 2\alpha_2\sqrt{t}$ where α_2 satisfies

$$e^{\alpha_2^2}\mathrm{erfc}(\alpha_2) = r^{-1} e^{r^2\alpha_2^2}\left[p_b^{-1}\hat{r} r^{-1} + \mathrm{erf}(r\alpha_2)\right], \tag{7}$$

otherwise no local maximum in the reaction rate occurs in zone 2. Thus, the condition for two local maxima in the reaction rate is

$$\hat{r} < \min(q^2 p_a^{-1}, r^2 p_b). \tag{8}$$

In Fig. 1, we illustrate reaction rate profiles with two local maxima, that satisfy Eq. (8), the parameter values $\kappa = \phi = p_a = p_b = r = 1$, $q = 1.1$ and $\hat{r} = 0.3$, at times $t = 0.02$, 0.04, 0.06, 0.08 and 0.1.

3.3. Small time moments of reaction rate

The definition of the position of the reaction front given by Chopard et al. [17] in dimensionless variables becomes

$$x_f = \frac{X_f}{l_0} = 2\sqrt{t}\frac{I_1}{I_0} \quad \text{where} \quad I_m = \int_{-\infty}^{0} \kappa a_0^{(1)} b_0^{(1)} \eta^m d\eta + \int_0^{\infty} a_0^{(2)} b_0^{(2)} \eta^m d\eta.$$

Using the small time asymptotic reactant profiles in Eq. (5) allows one to analytically evaluate these integrals to yield the position of the reaction front

$$x_f = \sqrt{\frac{t}{\pi}}\left(\frac{\frac{\pi}{2}\hat{r}p_b^{-1} + 1 + (r - r^{-1})\tan^{-1}(r) - \kappa[\frac{\pi}{2}p_a\hat{r}^{-1} + 1 + (q\hat{r}^{-1} - q^{-1}\hat{r})\tan^{-1}\left(\frac{q}{\hat{r}}\right)]}{\kappa(p_a + \sqrt{q^2 + \hat{r}^2} - \hat{r}) + \hat{r}p_b^{-1} + \sqrt{r^2 + 1} - 1}\right).$$

Notice, that the small time position of the reaction front x_f is independent of ϕ. The reaction front is initially stationary, i.e. $x_f = 0$, when $\kappa = \kappa_c$ where

$$\kappa_c = \frac{\frac{\pi}{2}\hat{r}p_b^{-1} + 1 + (r - r^{-1})\tan^{-1}(r)}{\frac{\pi}{2}p_a\hat{r}^{-1} + 1 + (q\hat{r}^{-1} - \hat{r}q^{-1})\tan^{-1}(\frac{q}{\hat{r}})}. \tag{9}$$

If $\kappa > \kappa_c$, the reaction front initially moves backwards to the left (zone 1), whilst if $\kappa < \kappa_c$ the reaction front initially moves forwards to the right (zone 2).

3.4. Large time asymptotic limit

In order to understand the dynamics of the whole system in time it is useful to know the large time asymptotic limit for this problem. Previously [28], we found that for large times the position of the reaction front is given by $x_f = 2\alpha\sqrt{t}$. If $r \geq \phi q$ then $\alpha \geq 0$ and α satisfies

$$re^{(r^2-1)\alpha^2}\mathrm{erfc}(r\alpha) = \phi[q + p_a\mathrm{erf}(\alpha)], \tag{10}$$

which, in the small α limit, yields the approximation

$$x_f \approx \frac{\sqrt{\pi t}(r - \phi q)}{r^2 + \phi p_a}.$$

Further, if $r < \phi q$ then $\alpha < 0$ and α satisfies

$$q\phi e^{(q^2-\hat{r}^2)\alpha^2}\mathrm{erfc}(-q\alpha) = r + p_b^{-1}\hat{r}\mathrm{erf}(-\hat{r}\alpha), \tag{11}$$

which in the small $|\alpha|$ limit yields the approximation

$$x_f \approx \frac{\sqrt{\pi t}(r - \phi q)}{p_b^{-1}\hat{r}^2 + \phi q^2}.$$

4. Numerical results

We can numerically solve the system of partial differential equations using a Crank-Nicolson finite difference scheme. A finite domain was chosen to be sufficiently large as to not affect the results and the mesh was chosen sufficiently fine that grid independent results were obtained. As this problem involves seven dimensionless parameters (κ, $\hat{r}$, ϕ, p_b, q, r and p_a) a full numerical parametric investigation is not feasible, however, an extensive numerical investigation found that the behaviour of the direction of the reaction front was much more exotic than the current literature presented it to be. In Fig. 2, we illustrate the position of the reaction front against the logarithm of time using the parameter values in set S with $\phi = 2$ for various values of r where

$$S = \left\{\kappa = \hat{r} = \frac{1}{2}, p_b = q = 2, p_a = 1\right\}.$$

Fig. 2 illustrates that the reaction front initially travels forwards, then backwards, and then if $4 < r \leq 4.267$ we find that the reaction front again travels forwards, then backwards, and finally forwards again, meaning that the reaction front has changed directions four times.

The small time asymptotic limit revealed that the reaction front initially moves forwards if $\kappa < \kappa_c$ where κ_c is given by Eq. (9). Substituting the parameter values in set S into Eq. (9) yields $\kappa_c \approx 0.7341$, so when $\kappa = 0.5$ the reaction front will initially move forwards. Using the parameter values in set S, the large time asymptotic limit reveals that the reaction front eventually moves forwards if $r > 4$.

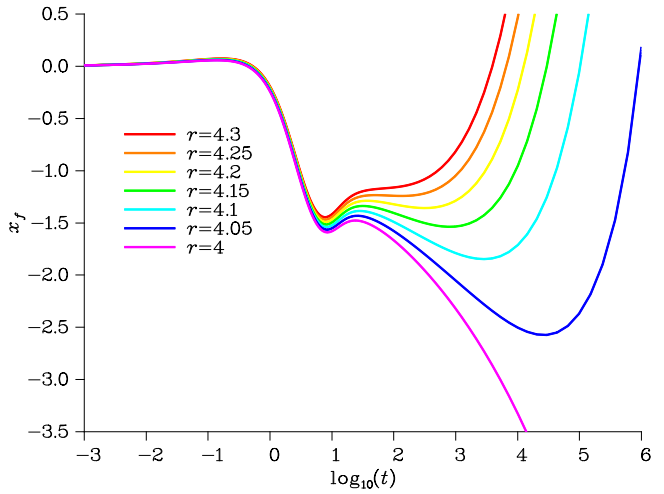

Fig. 2. Position of the reaction front x_f against the logarithm of time, $\log_{10}(t)$, using the parameter values in set S and $\phi = 2$ with r varying from 4 to 4.3.

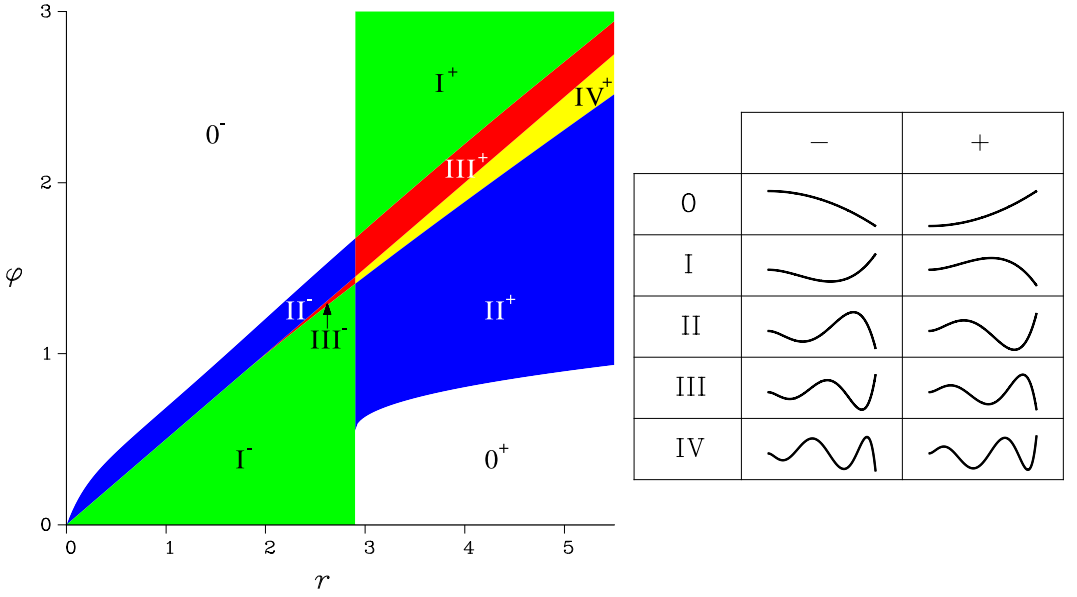

Fig. 3. Bifurcation diagram of the $(r,\ \phi)$ parameter space with the remaining parameters given in set S.

In Fig. 3, we illustrate the bifurcation diagram in the $(r,\ \phi)$ parameter space when the remaining parameter values are given in set S. Regions $0^{\pm}$, $\mathrm{I}^{\pm}$, $\mathrm{II}^{\pm}$, $\mathrm{III}^{\pm}$ and IV^{+} correspond to the number of times the reaction front changes direction and the $\pm$ corresponds to the initial direction of the reaction front, with $+$ denoting initially moves forwards and $-$ denoting initially moves backwards. We also illustrate the ten possible reaction front dynamics. The condition for a stationary reaction front in the small time asymptotic limit can be obtained by solving Eq. (9) using the values in set S, which yields the critical value $r_c = 2.899$. If $r < 2.899$, the reaction front initially moves backwards, but if $r > 2.899$, the reaction front initially moves forwards. The condition for a stationary reaction front in the large time asymptotic limit using the values in set S is $r = 2\phi$. If $r < 2\phi$ the reaction front eventually moves backwards, but if $r > 2\phi$ the reaction front eventually moves forwards.

If $r < 2.899$, for sufficiently large ϕ we are in region 0^- and the reaction front moves monotonically backwards. Decreasing ϕ sufficiently moves us into region II^- where the reaction front initially moves backwards, but changes directions twice and eventually moves backwards. If ϕ is decreased so that $\phi < 2r$ we cross into the narrow region III^- where the reaction front initially moves backwards, it will change directions three times and eventually move forwards. Decreasing ϕ sufficiently more we reach region I^- where the reaction front initially moves backwards but later in time changes direction to move forwards.

If $r > 2.899$, for sufficiently small ϕ we are in region 0^+ and the reaction front moves monotonically forwards. Increasing ϕ sufficiently moves us into region II^+ where the reaction front initially moves forwards, but changes directions twice and eventually moves forwards. If ϕ is increased sufficiently to reach region IV^+ where the reaction front initially moves forwards, it will change directions four times and eventually moves forwards. If ϕ is increased further so that $\phi > 2r$ we cross into region III^+ where the reaction front initially moves forwards, it will change directions three times and eventually moves backwards. Increasing ϕ sufficiently more we reach region I^+ where the reaction front initially moves forwards but later in time changes direction to move backwards.

We notice that the parameter values in set S do not yield the region IV^- which is absent from Fig. 3, however, by switching the roles or A and B we can create region IV^- but this would remove region IV^+.

5. Discussions and conclusions

In this study, we have analysed the properties of A+B→C reaction-diffusion fronts when the reactants A and B are initially dissolved in two different immiscible solvents. We find that, in this case, the reaction rate can in some cases feature two local maxima and there are ten possible types of reaction front dynamics. In particular, a reaction front can change directions four times. The main cause of this phenomenon is differential diffusion in the two phases. Early indications suggest that the region where the reaction front changes directions four times is located near the line $r = q\phi$. The purpose of this study was to highlight this exotic behaviour in the hope that there will be experimental studies to verify these unexpected predictions.

Data availability

No data was used for the research described in the article.

Acknowledgements

The authors thank Nathan Watts for many useful discussions. A.D. acknowledges financial support from Prodex and the ARC CREDI programme.

References

[1] P.J. Ortoleva, Geochemical Self-Organization, Oxford University Press, Oxford, 1994.
[2] J.D. Murray, Mathematical Biology, Springer Verlag, Berlin, 2003.
[3] I. Mastromatteo, B. Toth, J.P. Bouchaud, Anomalous impact in reaction-diffusion financial models, Phys. Rev. Lett. 113 (2014) 26870.
[4] P.V. Danckwerts, Unsteady-state diffusion or heat-conduction with moving boundary, Trans. Faraday Soc. 46 (1950) 701.
[5] G. Venzl, Pattern formation in precipitation processes. II. A postnucleation theory of Liesegang bands, J. Chem. Phys. 85 (1986) 2006.
[6] L. Gálfi, Z. Rácz, Properties of the reaction front in an $A + B \to C$ type reaction-diffusion process, Phys. Rev. A 38 (1988) 3151.
[7] S. Cornell, M. Droz, B. Chopard, Role of fluctuations for inhomogeneous reaction-diffusion phenomena, Phys. Rev. A 44 (1991) 4826.

[8] H. Larralde, M. Araujo, S. Halvin, H.E. Stanley, Reaction front for $A+B\to C$ diffusion-reaction systems with initially separated reactants, Phys. Rev. A. 46 (1992) 855.

[9] B. Chopard, M. Droz, T. Karapiperis, Z. Rácz, Properties of the reaction front in a reversible $A+B \underset{g}{\overset{k}{\rightleftharpoons}} C$ reaction-diffusion process, Phys. Rev. E 47 (1993) R40.

[10] Z. Koza, The long-time behavior of initially separated $A+B\to 0$ reaction-diffusion systems with arbitrary diffusion constants, J. Stat. Phys. 85 (1996) 179.

[11] J. Magnin, Properties of the asymptotic $nA+mB\to C$ reaction-diffusion fronts, Eur. Phys. J. B 17 (2000) 673.

[12] I. Hecht, H. Taitelbaum, Perturbation analysis for competing reactions with initially separated components, Phys. Rev. E 74 (2006) 012101.

[13] Y.-E.L. Koo, R. Kopelman, Space-and time-resolved diffusion-limited binary reaction kinetics in capillaries: Experimental observation of segregation, anomalous exponents, and depletion zone, J. Stat. Phys. 65 (1991) 893.

[14] H. Taitelbaum, Y.-E.L. Koo, S. Havlin, R. Kopelman, G.H. Weiss, Exotic behavior of the reaction front in the $A+B\to C$ reaction-diffusion system, Phys. Rev. A 46 (1992) 2151.

[15] S.H. Park, S. Parus, R. Kopelman, H. Taitelbaum, Gel-free experiments of reaction-diffusion front kinetics, Phys. Rev. E. 64 (2001) 055102.

[16] S.H. Park, H. Peng, R. Kopelman, H. Taitelbaum, Dynamical localization-delocalization transition of the reaction-diffusion front at a semipermeable cellulose membrane, Phys. Rev. E 75 (2007) 026107.

[17] B. Chopard, M. Droz, J. Magnin, Z. Rácz, Localization-delocalization transition of a reaction-diffusion front near a semipermeable wall, Phys. Rev. E 56 (1997) 5343.

[18] R. Tiani, L. Rongy, Complex dynamics of interacting fronts in a simple $A+B\to C$ reaction-diffusion system, Phys. Rev. E 100 (2019) 030201(R).

[19] Z. Koza, H. Taitelbaum, Motion of the reaction front in the $A+B\to C$ reaction-diffusion system, Phys. Rev. E. 54 (1996) R1040–R1043.

[20] H. Taitelbaum, Z. Koza, Anomalous kinetics of reaction diffusion fronts, Philosophical Magazine B 77 (1998) 1389–1400.

[21] H. Taitelbaum, Z. Koza, Reaction-diffusion processes: Exotic phenomena in simple systems, Physica A 285 (2000) 166.

[22] P.M.J. Trevelyan, Analytical small-time asymptotic properties of $A+B\to C$ fronts, Phys. Rev. E. 80 (2009) 046118.

[23] K. Eckert, A. Grahn, Plume and finger regimes driven by an exothermic interfacial reaction, Phys. Rev. Lett. 82 (1999) 4436.

[24] K. Eckert, L. Rongy, A. De Wit, $A+B\to C$ Reaction fronts in Hele-Shaw cells under modulated gravitational acceleration, Phys. Chem. Chem. Phys. 14 (2012) 7337.

[25] D.A. Bratsun, A. De Wit, On Marangoni convective patterns driven by an exothermic chemical reaction in two-layer systems, Phys. Fluids 16 (2004) 1083.

[26] D.A. Bratsun, A. De Wit, Buoyancy-driven pattern formation in reactive immiscible two-layer systems, Chem. Eng. Sci. 66 (2011) 5723.

[27] D.A. Bratsun, A. Mizev, V. Utochki, S. Nekrasov, A. Shmyrova, Nonlinear development of convective patterns driven by a neutralization reaction in immiscible two-layer systems, Phil. Trans. R. Soc. A 381 (2023) 20220178.

[28] P.M.J. Trevelyan, D.E. Strier, A. De Wit, Analytical asymptotic solutions of $nA+mB\to C$ reaction-diffusion equations in two-layer systems: A general study, Phys. Rev. E. 78 (2008) 026122.